Deep Mining 2024 – P Andrieux & D Cumming-Potvin (eds)

doi:10.36487/ACG_repo/2465_70

Application of the network connectivity index on fragmentation assessment in cave mine design

Yalin Li [a], Davide Elmo [a,*]

[a] *Norman B. Keevil Institute of Mining Engineering, The University of British Columbia, Canada*

Abstract

Cave mine design relies on reasonable fragmentation assessment to optimise production efficiency and minimise operational costs. In the past decade the volumetric fracture intensity (P_{32}) obtained from discrete fracture network (DFN) models has been widely used for fragmentation assessment in cave mine design. This paper examines the relationship between P_{32} and block sizes. The results show that P_{32} does not correlate well with key block size parameters D_{20}, D_{50}, and D_{80}, which are sizes at 20, 50 and 80% mass passing, respectively. As an alternative, the network connectivity index 3D (NCI_{3D}) is proposed as a geometric parameter to evaluate its correlation with block sizes. Results indicate that NCI_{3D} exhibits stronger associations with D_{20}, D_{50}, and D_{80} compared to P_{32}. Furthermore, NCI_{3D} can be a computationally efficient alternative to the traditional DFN-based block formation approach for evaluating fragmentation characteristics in cave mine design. This parameter could be applied to mine-scale DFN models for assessing localised fragmentation within various locations of the orebody.

Keywords: *network connectivity index, fracture intersection density, fracture, connectivity, discrete fracture network, fracture intensity, fragmentation assessment, cave mine*

1 Introduction

Fragmentation assessment is critical in cave mine designs. Specifically, rock fragments that are too large would result in hang-ups at the drawpoints, leading to a reduced production rate. Rock fragments that are too small would lead to ore loss and an inrush hazard at drawpoints. Both cases can significantly increase the operating cost and reduce the mine profit. Three stages of fragmentation in cave mines have been classified in the past decades: in situ fragmentation, primary fragmentation and secondary fragmentation (Brown 2007; Laubscher 1994). The assessment of in situ fragmentation directly influences the designs of preconditioning strategies (primary fragmentation) and draw columns (secondary fragmentation). However, it is impossible to recreate a physical twin (i.e. a prototype) of jointed rock masses in cave mines. Accordingly, the in situ fragmentation assessment in cave mine design is heavily relied on the discrete fracture network (DFN) approach.

DFN is widely used to model fractured rock masses. It involves explicitly representing geological fractures (e.g. joint, fault and bedding plane) as 2D discrete planes in a 3D space. The generation of fracture planes in the DFN model requires knowledge of spatial models and the statistical distributions of fracture frequency, fracture orientations and fracture radius. Those inputs can be obtained directly or through calculations from different field mapping techniques such as scanline and window mapping.

Fracture intensity is the widely accepted terminology in the DFN field to characterise the density of fractures in a DFN domain. The notation of fracture intensity is expressed as P_{ij}, where the subscript i refers to the dimension of the measurement region and the subscript j refers to the dimension of the sampling region. Several widely used fracture intensity parameters are listed:

* Corresponding author. Email address: davide.elmo@ubc.ca

- P_{10} represents the linear fracture intensity (number of fractures per unit length, dimensions m^{-1}).
- P_{20} is the fracture density (number of fractures per sampling area, dimensions m^{-2}).
- P_{21} represents the areal fracture intensity (sum of fracture length per sampling area, dimensions m^{-1}).
- P_{30} is the volumetric fracture density (number of fractures per sampling volume, dimensions m^{-3}).
- P_{32} represents the volumetric fracture intensity (sum of fracture area per sampling volume, dimensions m^{-1}).
- P_{21} can be directly mapped from rock exposures. Alternatively, it can also be estimated based on P_{10} using the following linear relationship:

$$P_{21} = C_{21} \times P_{10} \tag{1}$$

where C_{21} is the conversion constant. Its value depends on the fracture sizes and borehole orientations.

Estimation of P_{32} is challenging since it is a 3D parameter and cannot be directly mapped from rock exposure. For this reason, several studies (e.g. Chilès et al. 2008; Wang 2005; Ojeda et al. 2023) have proposed various approaches to estimate P_{32}. The most widely used and practical approach assumes that P_{32} has a linear relationship with P_{10}:

$$P_{32} = C_{31} \times P_{10} \tag{2}$$

It should be noted that P_{32} serves as an input to the DFN model. Therefore a validated P_{32} value requires an iterative trial-and-error process to match P_{10} from the geotechnical borehole data.

The in situ fragmentation assessment begins with developing reliable DFN models. However, the size of DFN models is typically small relative to that of the orebody due to computationally intensive block formation algorithms. For this reason, industry uses DFN models sized 10 × 10 × 10 m^3 to 15 × 15 × 15 m^3 to investigate the relationship between the volumetric intensity (P_{32}) and fragmentation. The geostatistical method is then used to interpolate P_{32} values for developing mine-scale geocellular models to assess in situ fragmentation (e.g. Munkhchuluun 2017; Rogers et al. 2015). This approach assumes that fracture orientation, size distribution, spatial models and fracture terminations are homogenous across the mine site.

This paper discusses that the fracture intensity alone is not ideal for in situ fragmentation assessment as it fails to capture the complex interactions and pathways that fractures create within the rock mass. An extensive set of DFN models based on 700 realisations has shown that P_{32} alone leads to a large variation in estimating key block size parameters D_{20}, D_{50} and D_{80} (i.e. block sizes at 20, 50 and 80% mass passing, respectively). In this study, the network connectivity index 3D (NCI_{3D}) developed by Elmo (2023) and Elmo et al. (2021) is proposed for block size assessment in cave mine design. It was found that NCI_{3D} can significantly reduce the variations of estimated block sizes and has the potential for application to fragmentation assessment for the cave mine design.

2 Network connectivity index

Fracture connectivity is widely used to study percolation problems and flow processes in rock masses. Despite its underlying potential, connectivity in rock engineering has always been confined to the periphery and the academic world. Zhang et al. (1992) developed a connectivity ratio to characterise natural rock fracture systems. It was found that the connectivity ratio is affected by size, density, pattern of fractures and the sampling area. Xu et al. (2006) proposed a connectivity index to account for the intersections of fractures in a mapping area. In their study, the connectivity index was used to characterise flow transport. They concluded that the connectivity index is a more suitable parameter to classify the flow characteristics of rock masses than fracture intensity parameters P_{21} and P_{32}. Alghalandis et al. (2015) proposed the

connectivity field to evaluate the spatial characteristics of fractures in the fracture network. Karimi Sharif et al. (2019) found that the same P_{21} may have different fracture intersection densities. For this reason, Karimi Sharif et al. (2019) proposed a visualisation technique for the interpretation of local fracture intersection density using the kernel density estimation method. These authors highlighted the importance of considering fracture connectivity and intersections for characterising rock mass conditions in many engineering applications.

Elmo et al. (2021, 2022) discussed the idea that fracture intensity alone is not ideal for characterising rock mass behaviour. The synthetic rock mass (SRM) models by Elmo & Stead (2010) show that for slender aspect ratios (width-to-height ratio, W:H, of less than 0.5) rock mass behaviour is sensitive to the relative fracture orientation concerning the loading. Anisotropic effects decrease with increasing W:H ratios and increasing P_{21}. However, isotropic conditions (baseline line assumption of common rock mass classification systems) are limited to W:H of two or higher, which is not the typical shape considered when assessing rock mass strength.

Using an extensive dataset of SRM models from three different mine sites and including different rock types, Elmo et al. (2021) proposed using connectivity parameters (the network connectivity index in 2D, abbreviated to NCI_{2D}) that combine areal fracture intensity (P_{21}), the number of fractures per unit area (P_{20}) and the number of intersections per area (I_{20}). The mathematical formulation of the NCI_{2D} is given by:

$$NCI_{2D} = \frac{P_{21}}{P_{20}} I_{20} \tag{3}$$

Compared to other existing connectivity parameters, the fracture intersection density I_{20} is calculated by accounting for both shape effects (W:H ratio) and censoring bias:

$$I_{20} = \frac{X_{int} + \frac{X_{top}}{W:H} + \frac{WX_{right}}{H} + \frac{WX_{left}}{H} + \frac{X_{bottom}}{W:H}}{Area} \tag{4}$$

In Equation 4, X_{int} is the number of fracture intersection points inside an areal mapping domain (2D), and X_{top}, X_{bottom}, X_{left} and X_{right} refer to the number of intersection points at the top, bottom, left and right boundaries of the mapping area, respectively. The width (W) and height (H) of the mapping area are used to adjust I_{20} to account for the shape of the mapping window relative to the direction of the major principal stress. The schematic of fracture intersections within a mapping window is shown in Figure 1.

Xu et al. (2006) and Huang et al. (2020) showed that the number of internal intersections (X_{int}) increases as P_{21} increases. While it is theoretically possible to use X_{int} as a simpler connectivity parameter than NCI, Equation 3 includes both P_{21} and I_{20} since i) the practice of determining P_{21} is beneficial for the eventual validation of the DFN model, and ii) SRM models may behave differently as a function of their relative W:H ratio and intersection density (including censored fractures at the boundary of the SRM model).

Elmo et al. (2022) proposed the use of the NCI_{2D} for quantifying the vertical (qualitative) axis of the geological strength index (GSI) chart by Hoek et al. (1995). The strengths of a large number of SRM models obtained from finite-discrete element method simulations (Elmo 2006; Elmo et al. 2021) were normalised to the intact rock strength and plotted against the NCI_{2D}. The equivalent GSI rating back-calculated based on SRM strength was then correlated with the NCI_{2D} to develop the modified GSI table shown in Figure 2. Note that in Figure 2 the modified ranges of GSI were introduced by Elmo et al. (2022) following the work by Marinos & Carter (2018) to better incorporate geology into GSI and account for the irreversibility problem discussed in Elmo & Stead (2021). It is not necessary to seek a precise NCI_{2D} rating due to the stochastic nature of the parameters in Equation 3. Following an extensive sensitivity analysis to study the impact of the parameters used to calculate the NCI, Fogel (2022) suggested using $NCI_{2D} \pm 1$.

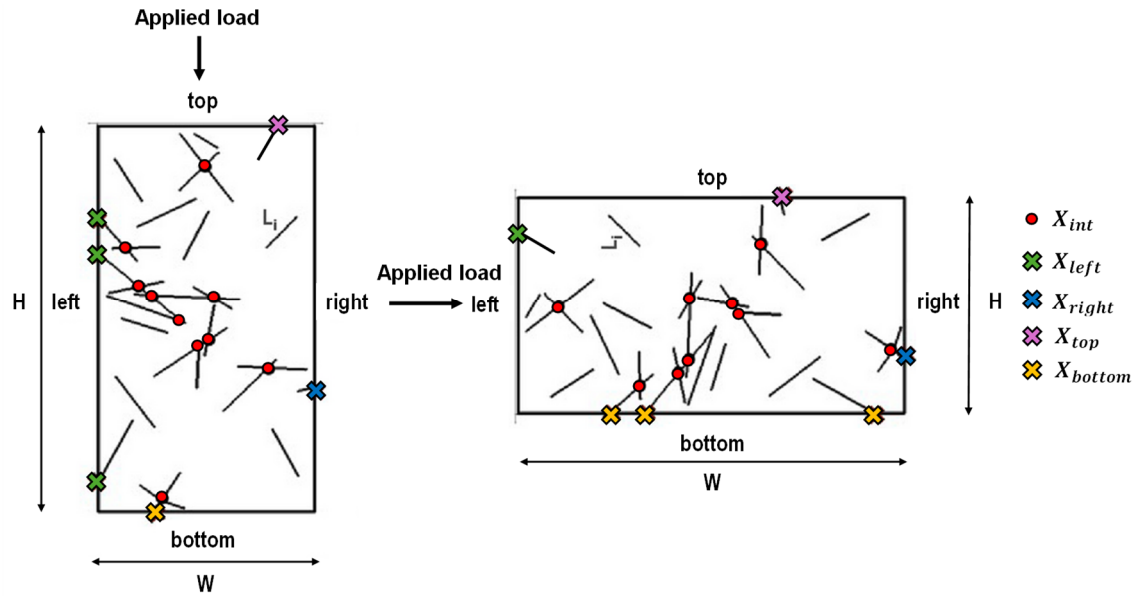

Figure 1 Schematic for X_{int}, X_{left}, X_{right}, X_{top} and X_{bottom} within a mapping window for a 2D network connectivity index calculation after Elmo et al. (2021)

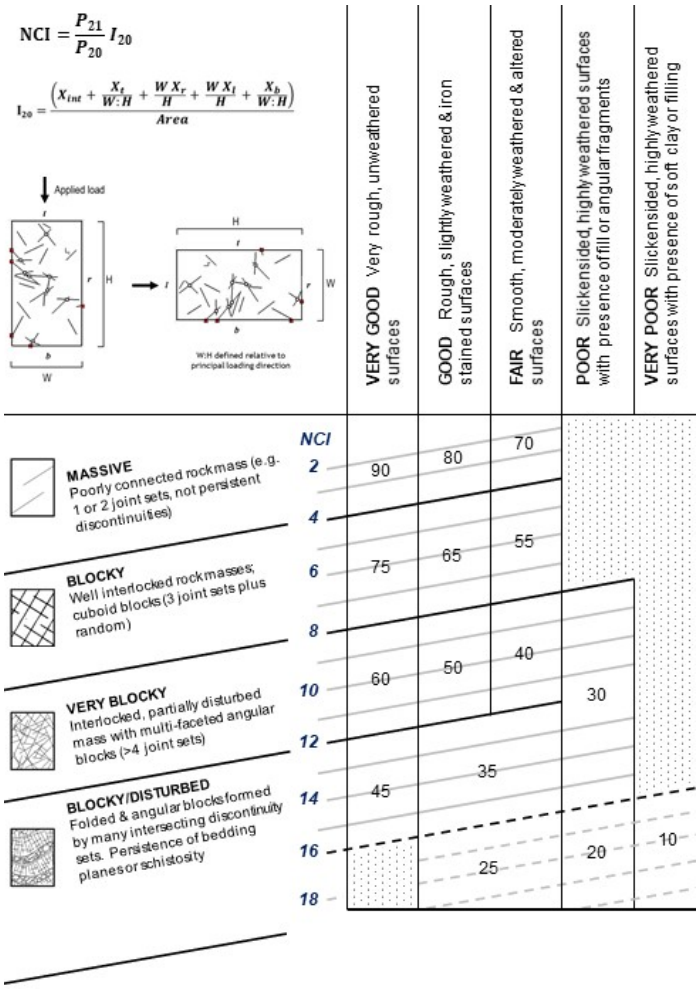

Figure 2 2D network connectivity index classification ratings superimposed onto the modified geological strength index classification table by Elmo et al. (2022)

Elmo (2023) investigated the applications of the NCI_{2D} to study rock bridge strength instead of using the much-limited approach by Jennings (1970). The author introduced the concept of rock bridge potential, which treats rock bridge strength as simply a manifestation of rock mass strength. According to Elmo (2023), a rock bridge is defined as the portion of intact rock between discontinuity surfaces that has the potential to fail under certain stress conditions. Quoting the same author, 'Before failure, it is not a matter of describing rock bridges as physical entities. There are only potential rock bridges that exist everywhere at once. Only when the rock mass has failed it is possible to determine the position and extent of the rock bridges'.

The rock bridge (rb) potential is defined as the ratio between the $NCI_{2D,rb}$ and the summation of the NCI_{2D} and $NCI_{2D,\ rb}$ given by:

$$Rock\ bridge\ potential = \frac{NCI_{2D}}{NCI_{2D} + NCI_{2D,rb}} \tag{5}$$

where $NCI_{2D,rb}$ represents the NCI of the induced fractures.

Figure 3 illustrates the use of the rock bridge potential to characterise rock mass behaviour. The objective is to use Equation 5 to describe whether the failure is governed by stress-induced phenomena (e.g. spalling) or occurs due to structurally controlled mechanisms or as a combination. Using results from Elmo (2023) (Models A1 and A2 in Figure 3, SRM models investigating resistance under shear loading conditions), rock mass behaviour is described concerning the maximum shear stress at failure normalised to intact cohesive strength and the proportional contribution of stress-driven failure (represented by $NCI_{2D,\ rb}$) and structurally controlled failure (represented by the initial NCI_{2D}). Interestingly, Models A1 and A2 have very similar NCI_{2D} but behave very differently due to the presence of a major structure along the failure direction.

Elmo (2023) conceptualised a 3D formulation for the NCI (NCI_{3D}), expressed as:

$$NCI_{3D} = \frac{P_{32}}{P_{30}} I_{30} \tag{6}$$

The volumetric intersection density I_{30} (i.e. number of intersection lines per volume) was not proposed in the original work. This study attempted to use the NCI_{3D} as a geometric parameter for fragmentation assessment in cave mines design. The formulation of I_{30} is given below:

$$I_{30} = \frac{X_{int} + X_{top} + X_{bottom} + X_{left} + X_{right} + X_{front} + X_{back}}{Volume} \tag{7}$$

where X_{int} is the number of fracture intersection lines inside a 3D cubic domain, and X_{top}, X_{bottom}, X_{left}, X_{right}, X_{front} and X_{back} refer to the numbers of intersection lines at the cubic domain top, bottom, left, right, front and back faces, respectively. Note that the proposed I_{30} formulation assumes cubic volume regions. Therefore the shape adjustment factor (W:H) used in I_{20} is no longer required. More importantly, the shape adjustment factor reflects the relative impact of loading direction with respect to terminations and fracture orientation (i.e. interlocking potential). In situ fragmentation analyses are not geomechanical models; therefore loading assumptions are not required. In this next section an extensive dataset of DFN models is developed to examine the use of fracture intensity and the NCI_{3D} on in situ fragmentation assessment.

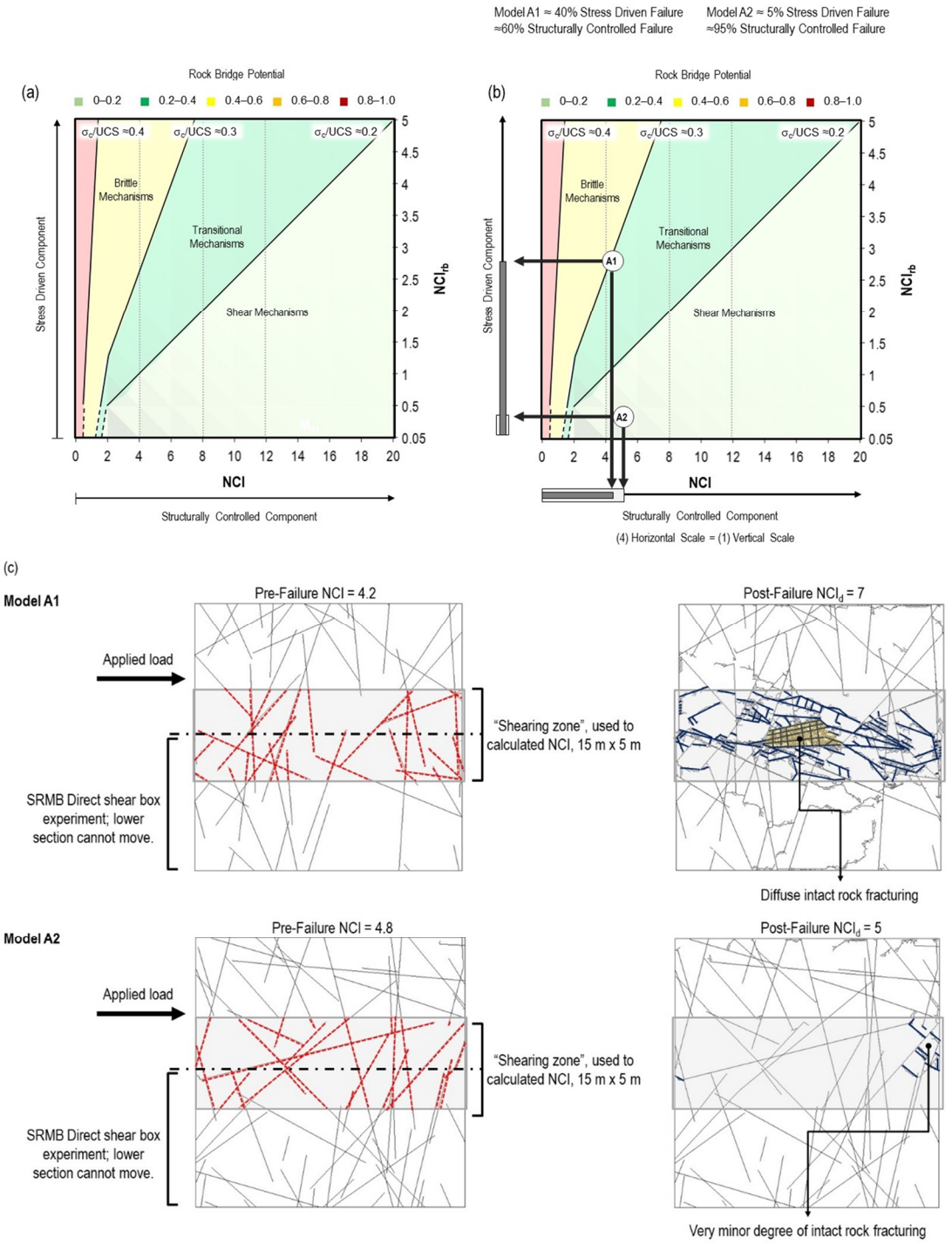

Figure 3 (a) Network connectivity index in 2D approach for characterising rock bridge potential and failure mechanisms (modified from Bewick & Elmo 2024); (b) Example for the models shown in (c)

3 Fragmentation assessment in cave mines

3.1 Discrete fracture network-based block formation

The block size generated based on the DFN model has been used in various rock and mining engineering applications. There are two main types of DFN-based block formation algorithms: explicit and implicit (Elmo et al. 2014). The explicit block formation algorithm generates blocks with their faces accurately intersected by the fracture network. In some instances (e.g. 3DEC [ITASCA 2019], Unblocks^{gen} [Rasmussen 2020]) the

explicit block formation algorithm is used in combination with the assumptions of fully persistent and continuous fractures to avoid generating blocks with complicated geometries (i.e. concave blocks).

The implicit block formation algorithm overlays a fine and cubic grid of cells in the DFN domain, which is followed by a joining up the cells not separated by fractures to assemble blocks. The implicit algorithm considers actual fracture sizes and can form blocks with complex geometries. The fragmentation grid (FG) approach (also called Sybil Frac) available in the commercial DFN program *FracMan* (WSP 2021) employs an implicit block formation algorithm. As expected, grid cell density (i.e. the number of cells) is known to impact size distribution curves, particularly in smaller block sizes. Characterisation of smaller block sizes improves with decreasing cell size and thus requires an increasing number of grid cells for the same problem scale. The process becomes computationally intensive for very fine grids and may not be practical for assessing fragmentations in multiple realisations. A maximum density of 150 × 150 × 150 grid cells is generally used (WSP 2021). Using this maximum density and assuming hypothetical rock volumes of 15 × 15 × 15 m^3 and 30 × 30 × 30 m^3 rock mass, the minimum block size would be 1E-3 m^3 and 8E-3 m^3, respectively.

Figure 4 shows the comparisons of block size distribution curves generated by 3DEC and *FracMan* using the same DFN model. The results show that the portion of block sizes at higher percentage mass passing (i.e. >50% mass passing) generated from 3DEC is smaller than that from *FracMan*. At low percentage mass passing, *FracMan* estimates higher block sizes than 3DEC. This is due to the aforementioned limitation that the minimum grid size parameters affect the accuracy of smaller block size predictions. Furthermore, it was found that smaller blocks with irregular shapes (i.e. thin or have high aspect ratios) cannot be reasonably represented by cubic grids.

Despite the limitation of the FG approach on estimating small and irregular-shaped blocks, the approach would be suitable for in situ fragmentation assessment. Estimating larger block sizes at high percentage mass passing for in situ fragmentation would lead to a more conservative preconditioning design. Since the focus of the NCI_{3D} application is on cave mine applications, the FG approach in *FracMan* is implemented to assess the block sizes of each realisation in the synthetic DFN dataset.

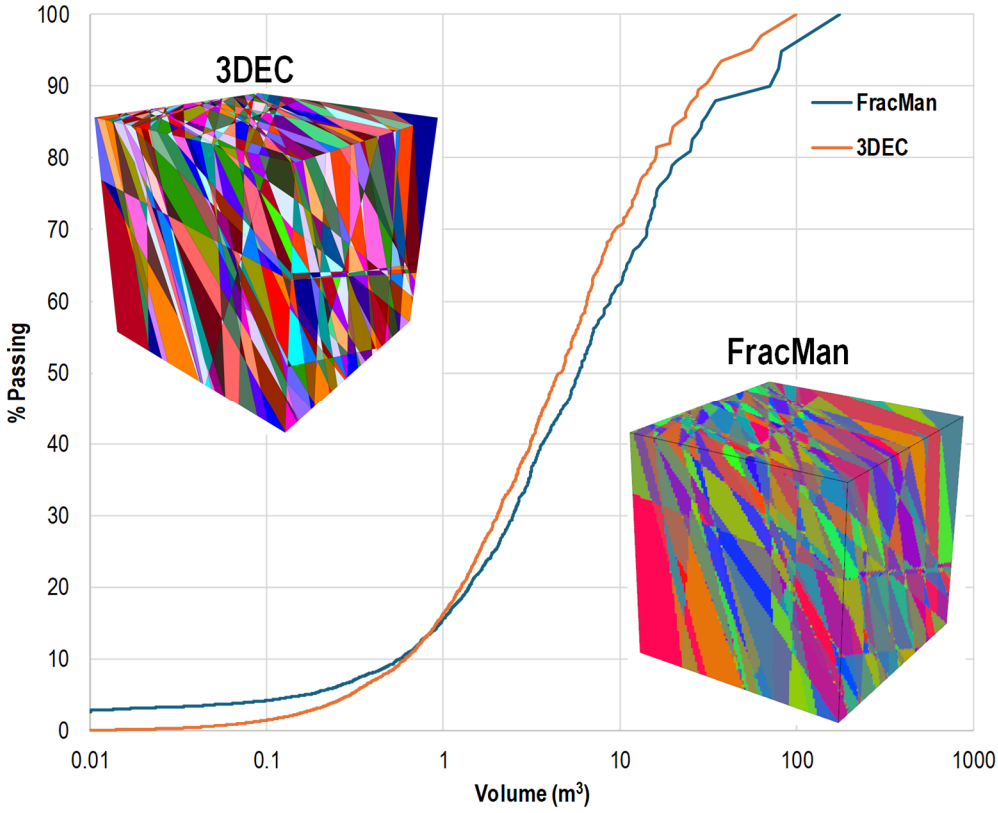

Figure 4 Comparison of block size distribution curves generated by 3DEC and *FracMan*

3.2 Synthetic dataset

The study used 700 synthetic DFN realisations to compare fracture intensity P_{32} and the NCI_{3D} for in situ fragmentation assessment. The Fisher distribution generated fractures with various orientations using the disaggregate approach for each realisation. Figure 5 shows the stereonet contours of Fisher K of 1, 5 and 10, and mean fracture orientations of 000/90 and 030/60 (pole trend/plunge) used to generate the synthetic data. Furthermore, two fracture sizes were considered in the generation of a synthetic dataset in each scenario shown in Figure 5: persistent fractures (i.e. average fracture radius of 30 m) and non-persistent fractures (i.e. lognormal distribution with a mean fracture radius of 5 m and standard deviation of 0.5 m, truncated at 0.25 and 15 m). P_{32} values as input parameters in the synthetic data range from 0.75 to 3.75 m^{-1}. Ten realisations were generated for each combination of Fisher K, mean fracture orientation and fracture size to account for variabilities.

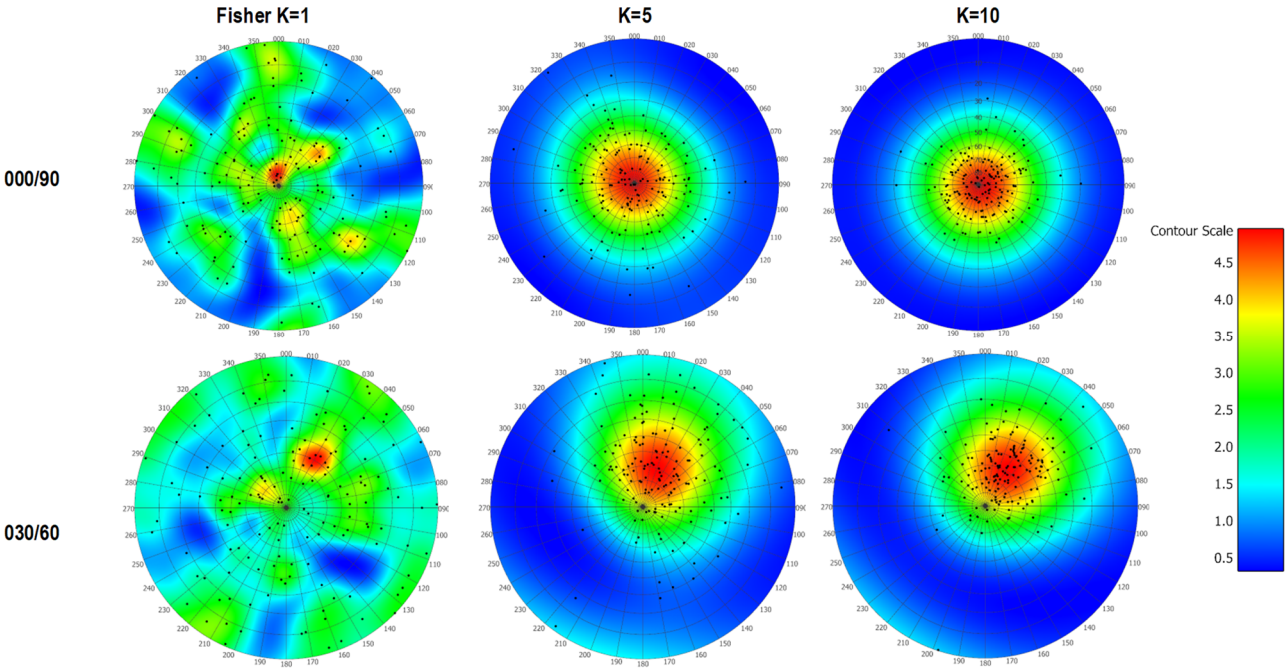

Figure 5 Discrete fracture network realisations with various fracture orientations and Fisher K

Figure 6 shows the process used in the analysis for block search and intersection calculations. The workflow of the study is illustrated in Figure 7. For each DFN realisation shown in Figure 6a, the block sizes were assessed using the FG method shown in Figure 6b. Fracture-to-fracture intersection lines inside the domain (Figure 6c) and fracture-domain boundary intersection lines (Figure 6d) are then computed. Note that in the code *FracMan*, the intersection lines shown in Figures 6c and 6d are treated as polylines formed by adjoining segments; adjoining nodes need to be removed when determining the full length of the intersection line. For each realisation the computed NCI_{3D} was compared to key block size parameters D_{20}, D_{50} and D_{80}.

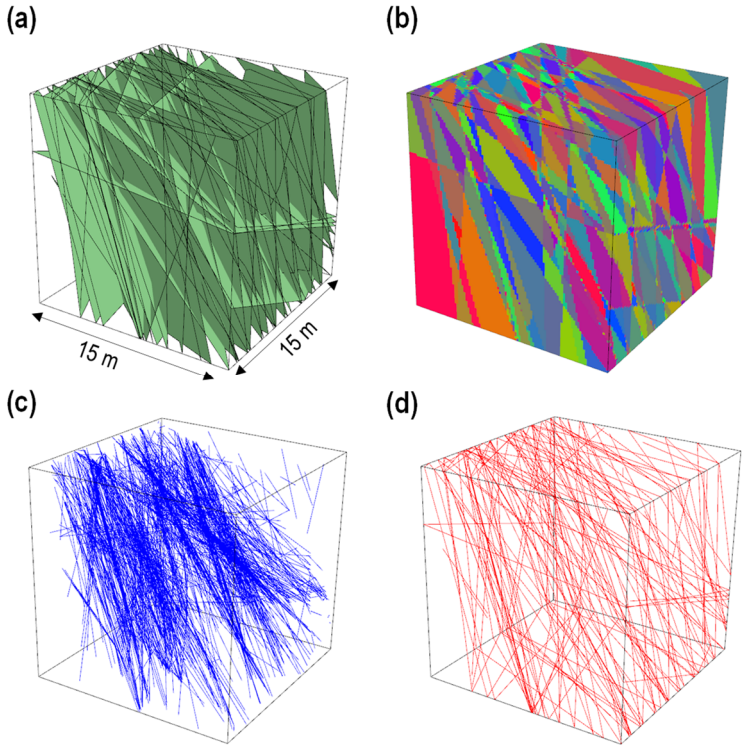

Figure 6 (a) Generated discrete fracture network model; (b) Mapped blocks; (c) Fracture intersections inside the domain; (d) Fracture intersections at domain boundaries

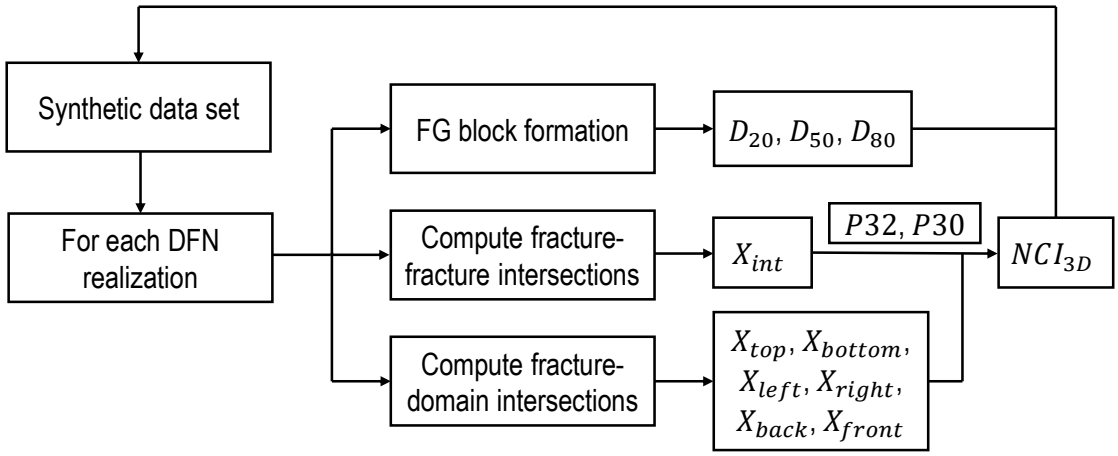

Figure 7 Procedures for computing the 3D network connectivity index and fragmentation for each realisation in the synthetic model

3.3 Comparison of volumetric fracture intensity and the 3D network connectivity index for in situ fragmentation assessment

Figure 8 shows D_{20}, D_{50} and D_{80} plotted against P_{32}. Power functions fitted to relate block sizes and P_{32} show that the same P_{32} can correspond to large variations in block sizes (D_{50} and D_{80}). Unreasonable estimations of block sizes at higher percentage mass passing may lead to inappropriate preconditioning design if feasibility of the preconditioning is strictly associated to the presence of larger blocks in situ. This problem is resolved when using the NCI_{3D} (Figure 9). Differences observed concerning the power curve for D_{20} can be explained taking into consideration the limitations of the implicit block size search in *FracMan*, which may not capture blocks that are too small relative to the minimum grid cell size. Overall, the results show a reasonable correlation between block sizes and the NCI_{3D}, and confirm the advantage of using fracture connectivity over fracture intensity to characterise rock mass fragmentation (blockiness).

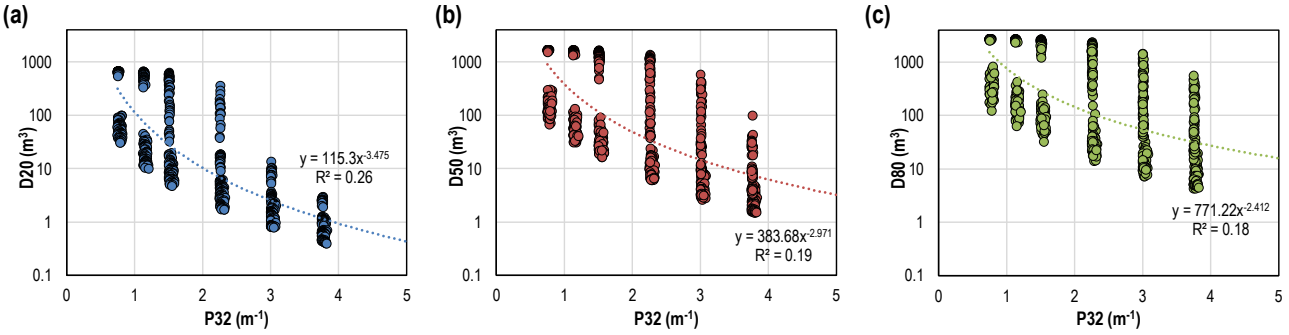

Figure 8 **Block size at 20, 50 and 80% of mass passing plotted against volumetric fracture intensity**

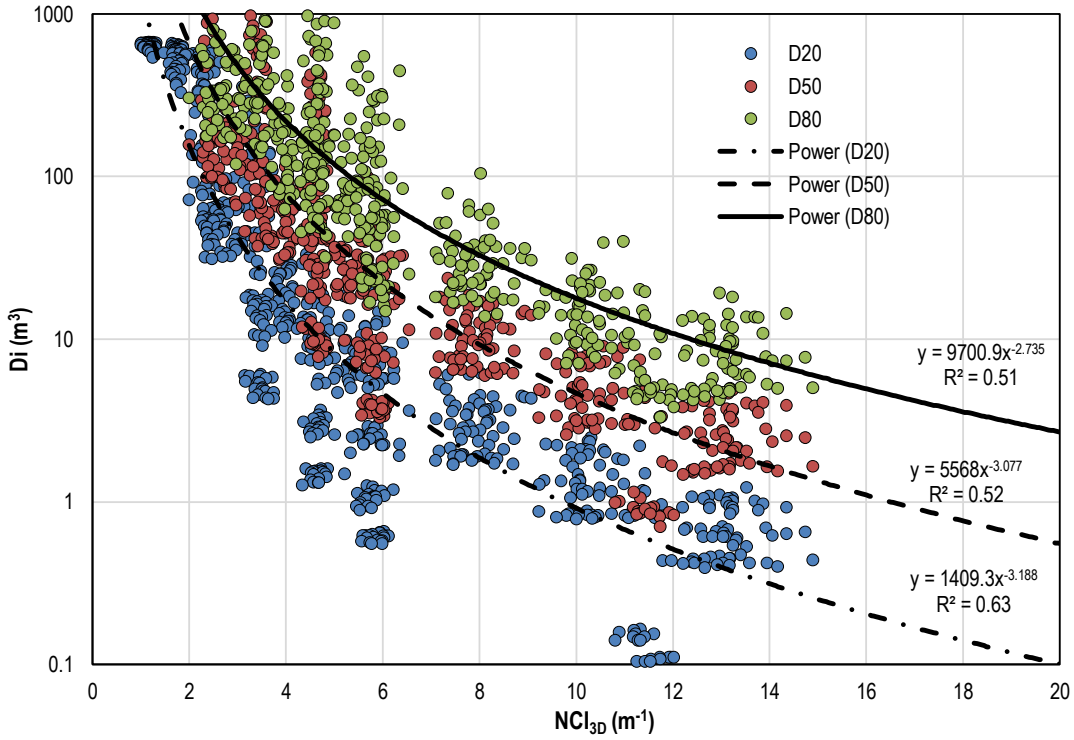

Figure 9 **Block size at 20, 50 and 80% of mass passing plotted against the 3D network connectivity index**

4 Implications of the 3D network connectivity index for mine-scale fragmentation assessment

Elmo et al. (2014) developed a mine-scale DFN model for in situ fragmentation assessment (Figure 10). The DFN model was developed based on fractures along boreholes from the pit shell (Figures 10a, b and c). The grids were created within the DFN domain and P_{32} within each grid was computed (Figure 10d). As discussed in Section 3.1, the accuracy of results from the implicit block formation algorithm is heavily relied upon for the density of overlaid grids. Using the implicit algorithm in such large-scale DFN model is computationally intensive and may lead to inaccurate results. Therefore, in the analysis by Elmo et al. (2014), the fragmentation assessment was limited within a 15 × 15 × 15 m domain and block size distributions were related to P_{32}.

It has been discussed that P_{32} for fragmentation assessment may lead to large variations for estimating large blocks, which could result in less conservative preconditioning design. The NCI_{3D} presented in this study reduces the variation for estimating block sizes and can be suitable in such mine-scale DFN models for assessing fragmentation within the orebody. The computation for fracture-fracture intersections is less intensive than explicit and implicit block formation algorithms. The NCI_{3D} has potential to replace P_{32} for assessing localised fragmentation in the mine-scale DFN model with multiple realisations.

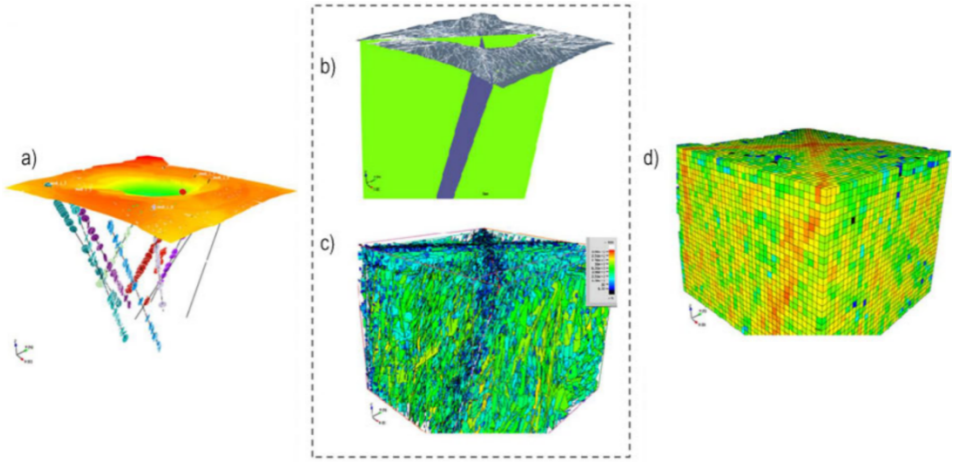

Figure 10 A mine-scale discrete fracture network model: (a) Pit shell and a number of the boreholes used for bootstrapping the fracture orientations from (b); (c) Discrete fracture network model containing both stochastically generated and deterministically placed major structures; (d) Computation of the model's resultant volumetric fracture intensity property (Elmo et al. 2014)

5 Conclusion and future research

This paper has reviewed the use of DFN modelling and fracture intensity in rock and mining engineering applications, and discussed that P_{32} alone is not ideal for fragmentation assessment in cave mine design. An extensive dataset of 700 DFN realisations with various fracture orientations, Fisher K and fracture sizes has shown that estimations of block sizes using P_{32} may lead to large variations. This could result in unconservative preconditioning design in cave mines. To overcome this limitation, this study proposed that the NCI_{3D} be treated as a geometry parameter for fragmentation assessments. It has been found that the NCI_{3D} correlates better with block sizes than with P_{32}, which can serve as a more representative parameter for fragmentation assessment. Compared to traditional DFN-based block formation algorithms, the NCI_{3D} provides a more practical solution for assessing localised fragmentation in mine-scale DFN models as the computation of fracture intersections is less intensive the block formation algorithms.

Future research will explore the applications of the NCI_{3D} in rock mass classification, rock bridge potential and primary fragmentation assessment, integrating an analysis of how principal stress orientation and magnitude, as well as rock strength, influence rock mass behaviour and fragmentation in various rock and mining engineering applications.

Acknowledgement

The authors wish to acknowledge the Mitacs grant in collaboration with the Centre of Innovation in Mineral Resource Engineering and Newcrest Mining Limited for the financial support provided to this research.

References

Alghalandis, YF, Dowd, PA, & Xu, C 2015, 'Connectivity field: a measure for characterising fracture networks', *Mathematical Geosciences*, vol. 47, no. 1, pp. 63–83.

Bewick, RP & Elmo, D 2024, 'Failure mechanism dependency of rock mass strength', *Rock Mechanics and Rock Engineering*, under review.

Brown, E 2007, *Block Caving Geomechanics*, Julius Kruttschnitt Mineral Research Centre, The University of Queensland, Indooroopilly.

Chilès, J-P, Wackernagel, H, Beucher, H, Lantuéjoul, C & Elion, P 2008, 'Estimating fracture density from a linear or aerial survey', in J Ortiz & X Emery (eds), *Proceedings of the VIII International Geostatistics Congress*, Gecamin, Santiago, pp. 535–544.

Elmo, D 2006, *Evaluation of a Hybrid FEM/DEM Approach for Determination of Rock Mass Strength Using a Combination of Discontinuity Mapping and Fracture Mechanics Modelling, With Particular Emphasis on Modelling of Jointed Pillars*, PhD thesis, University of Exeter.

Elmo, D 2023, 'The Bologna interpretation of rock bridges', *Geosciences*, vol. 13, no. 2.

Elmo, D, Rogers, S, Stead, D & Eberhardt, E 2014, 'Discrete fracture network approach to characterise rock mass fragmentation and implications for geomechanical upscaling', Mining Technology, vol. 123, no. 3, pp. 149–161.

Elmo, D & Stead, D 2010, 'An integrated numerical modelling–discrete fracture network approach applied to the characterisation of rock mass strength of naturally fractured pillars', *Rock Mechanics and Rock Engineering*, vol. 43, pp. 3–19.

Elmo, D & Stead, D 2021, 'The role of behavioural factors and cognitive biases in rock engineering', *Rock Mechanics and Rock Engineering*, vol. 54, pp. 2109–2128.

Elmo, D, Stead, D, Yang, B, Marcato, G & Borgatti, L 2022, 'A new approach to characterise the impact of rock bridges in stability analysis', *Rock Mechanics and Rock Engineering*, vol. 55, no. 5, pp. 2551–2569.

Elmo, D, Yang, B, Stead, D & Rogers, S 2021, 'A discrete fracture network approach to rock mass classification', in M Barla, A Di Donna & D Sterpi (eds), *Challenges and Innovations in Geomechanics: Proceedings of the 16th International Conference of IACMAG – Volume 1*, Springer, Berlin, pp. 854–861.

Fogel, Y 2022, *A Sensitivity Analysis for the Network Connectivity Index (NCI) Using Discrete Fracture Networks (DFN)*, PhD thesis, The University of British Columbia, Vancouver, http://dx.doi.org/10.14288/1.0422909

Hoek, E, Kaiser, PK & Bawden, WF 1995, *Support of Underground Excavations in Hard Rock*, CRC Press, Boca Raton.

Huang, F, Yao, C, Yang, J, He, C, Shao, Y & Zhou, C 2020, 'Connectivity evaluation of fracture networks considering the correlation between trace length and aperture, *Applied Mathematical Modelling*, vol. 88, pp. 870–887.

ITASCA 2019, *3DEC (3 Dimensional Distinct Element Code)*, version 7.0, computer software, https://www.itasca.com.au/software/3dec

Jennings, J 1970, 'A mathematical theory for the calculation of the stability of slopes in open cast mines', in P van Rensburg (ed.), *Planning Open Pit Mines: Proceedings of the Symposium on the Theoretical Background to the Planning of Open Pit Mines with Special Reference to Slope Stability*, pp. 87–102.

Karimi Sharif, LK, Elmo, D & Stead, D 2019, 'Improving DFN-geomechanical model integration using a novel automated approach', *Computers and Geotechnics*, vol. 105, pp. 228–248.

Laubscher, D 1994, 'Cave mining-the state of the art', *Journal of The Southern African Institute of Mining and Metallurgy*, vol. 94, no. 10, pp. 279–293.

Marinos, V & Carter, TG 2018, 'Maintaining geological reality in application of GSI for design of engineering structures in rock', *Engineering Geology*, vol. 239, pp. 282–297.

Munkhchuluun, M 2017, *Linking the Fracture Intensity of an In Situ Rock Mass to Block Cave Mine Fragmentation*, PhD thesis, The University of British Columbia, Vancouver.

Ojeda, P, Elmo, D, Rogers, S & Brzovic, A 2023, 'Discrete fracture network (DFN) analysis to quantify the reliability of borehole-derived volumetric fracture intensity', *Geosciences*, vol. 13, no. 6, https://doi.org/10.3390/geosciences13060187

Rasmussen, LL 2020, 'UnBlocks^{gen}: A Python library for 3D rock mass generation and analysis', *SoftwareX*, vol. 12, https://doi.org/10.1016/j.softx.2020.100577

Rogers, S, Elmo, D, Webb, G & Catalan, A 2015, 'Volumetric fracture intensity measurement for improved rock mass characterisation and fragmentation assessment in block caving operations', *Rock Mechanics and Rock Engineering*, vol. 48, pp. 633–649.

Wang, X 2005, *Stereological Interpretation of Rock Fracture Traces on Borehole Walls and Other Cylindrical Surfaces*, PhD thesis, Virginia Tech, Blacksburg.

WSP 2021, *FracMan*, version 8.0, computer software, https://www.wsp.com/en-au/services/fracman

Xu, C, Dowd, P, Mardia, K & Fowell, R 2006, 'A connectivity index for discrete fracture networks', *Mathematical Geology*, vol. 38, pp. 611–634.

Zhang, X, Harkness, RM & Last, NC 1992,' Evaluation of connectivity characteristics of naturally jointed rock masses', *Engineering Geology*, vol. 33, no. 1, pp. 11–30.